

Anti-*Leishmania* compounds can be screened using *Leishmania* spp. expressing red fluorescence (*tdTomato*)

Mariza Gabriela Faleiro de Moura Lodi Cruz,^{1,2} Ana Maria Murta Santi,¹ Eliane de Moraes-Teixeira,³ Alisson Samuel Portes Caldeira,² Ezequias Pessoa de Siqueira,² Edward Oliveira,¹ Tânia Maria de Almeida Alves,² Silvane Maria Fonseca Murta¹

AUTHOR AFFILIATIONS See affiliation list on p. 19.

ABSTRACT The main challenges associated with leishmaniasis chemotherapy are drug toxicity, the possible emergence of resistant parasites, and a limited choice of therapeutic agents. Therefore, new drugs and assays to screen and detect novel active compounds against leishmaniasis are urgently needed. We thus validated *Leishmania braziliensis* (Lb) and *Leishmania infantum* (Li) that constitutively express the tandem tomato red fluorescent protein (*tdTomato*) as a model for large-scale screens of anti-*Leishmania* compounds. Confocal microscopy of Lb and Li::tdTomato revealed red fluorescence distributed throughout the entire parasite, including the flagellum, and flow cytometry confirmed that the parasites emitted intense fluorescence. We evaluated the infectivity of cloned promastigotes and amastigotes constitutively expressing *tdTomato*, their growth profiles in THP-1 macrophages, and susceptibility to trivalent antimony, amphotericin, and miltefosine *in vitro*. The phenotypes of mutant and wild-type parasites were similar, indicating that the constitutive expression of *tdTomato* did not interfere with the evaluated parameters. We applied our validated model to a repositioning strategy and assessed the susceptibility of the parasites to eight commercially available drugs. We also screened 32 natural plant and fungal extracts and 10 pure substances to reveal new active compounds. The infectivity and Glucantime treatment efficacy of BALB/c mice and golden hamsters infected with Lb and Li::tdTomato mutant lines, respectively, were very similar compared to animals infected with wild-type parasites. Standardizing our methodology would offer more rapid, less expensive, and easier assays to screen of compounds against *L. braziliensis* and *L. infantum* *in vitro* and *in vivo*. Our method could also enhance the discovery of active compounds for treating leishmaniasis.

KEYWORDS *Leishmania*, *tdTomato*, compound screening, chemotherapy, natural products

Leishmaniasis is an infectious disease caused by protozoan parasites of the genus *Leishmania* (1). It is classified as a neglected tropical disease but is of great importance to public health over a wide geographical distribution (1, 2). Estimates indicate that leishmaniasis affects 12 million people worldwide, and ~1 billion live in at-risk areas, where the annual incidence is ~2 million (1). The parasites are transmitted to vertebrate hosts through bites by infected female sandflies from various species of the genera *Phlebotomus* and *Lutzomyia* (2, 3). *Leishmania* is a unicellular organism that morphologically exists as a flagellate, mobile promastigote in the gut of vector insects and a non-flagellated, immobile, intracellular amastigote found in cells of the phagocytic monocytic system of vertebrate hosts (3). The two main clinical forms of leishmaniasis are tegumentary, characterized by cutaneous and mucosal lesions, and visceral (VL), in which the parasites have tropism for internal organs such as the liver, spleen, and bone marrow (2, 3). The visceral form causes the most severe leishmaniasis, which can

Editor Audrey Odom John, The Children's Hospital of Philadelphia, Philadelphia, Pennsylvania, USA

Address correspondence to Tânia Maria de Almeida Alves, tania.alves@focruz.br, or Silvane Maria Fonseca Murta, silvane.murta@focruz.br.

Mariza Gabriela Faleiro de Moura Lodi Cruz and Ana Maria Murta Santi contributed equally to this article. Author order was determined both alphabetically and in order of increasing seniority.

The authors declare no conflict of interest.

See the funding table on p. 19.

Received 20 April 2023

Accepted 30 October 2023

Published 8 December 2023

Copyright © 2023 American Society for Microbiology. All Rights Reserved.

be lethal if untreated. *Leishmania (Viannia) braziliensis* (Lb) and *Leishmania (Leishmania) infantum* (Li) are epidemiologically relevant and cause cutaneous and visceral leishmaniasis, respectively (1).

The absence of vaccines for humans and effective vector control programs has led to chemotherapy being the primary strategy for controlling all forms of leishmaniasis. Only a few drugs to treat leishmaniasis are available, namely, pentavalent antimonials such as sodium stibogluconate and meglumine antimoniate, amphotericin B formulations (deoxycholate and liposomal), miltefosine, paromomycin sulfate, and pentamidine isethionate (4). However, the high toxicity of these drugs, the possible emergence of resistant parasites, and the limited choice of drugs are the main challenges associated with chemotherapy (5). Therefore, the need to discover new drugs and new ways to screen and detect novel active compounds against leishmaniasis is urgent.

Various experimental models for screening drugs to treat leishmaniasis *in vitro* and *in vivo* have been described (6–10). *In vitro* models using intracellular amastigotes are more suitable for drug screening against *Leishmania* due to clinical relevance but cannot predict all the *in vivo* events. On the other hand, we still do not have a standard and universal model for anti-*Leishmania* drug screenings, and the models differ in immune responses and clinical symptoms (6–10).

The first *in vitro* assays involved manually counting intracellular amastigotes, which was laborious and difficult to scale up for high-throughput screening (11). A high-content assay using cell imaging of *L. donovani* parasites was later validated. This assay allowed simultaneous measurements of compound effectiveness against intracellular amastigotes and toxicity to human macrophages (12).

Current assays using *Leishmania* parasites expressing recombinant reporter genes including *Escherichia coli* galactosidase (lacZ) (13), β -lactamase (14), firefly luciferase (15), and green fluorescent protein (GFP) (16) have specific advantages and disadvantages (6, 16). Colorimetric assays are rapid and simple and work by adding an enzyme substrate, which causes a color change of the medium according to cell metabolism and viability. However, colored compounds can interfere with the readout of colorimetric substrates, and enzyme activity can only be measured at a single endpoint (12). Luminescence detection is sensitive and reproducible on a large scale but adding a detection substrate significantly increases the cost of such tests (17–19). GFP and red fluorescent protein (RFP), mCherry, and *tdTomato* proteins have been applied to test the actions of compounds/drugs against *Leishmania* spp. Although GFP can be expressed in *Leishmania* spp. (20–22), its fluorescence emission (509 nm) is similar to the macrophage autofluorescence, which can be also detected by fluorescein isothiocyanate (FITC) or PE channel (FL1), limiting its utility to assessing the susceptibility of intracellular amastigotes (23, 24). On the other hand, among the several red fluorescent proteins derived from *Discosoma coral*, *tdTomato* is the most photostable and the brightest. This renders it easily detectable *in vitro* and *in vivo* (25) by fluorimetry or flow cytometry. Furthermore, *tdTomato* fluorescence has values excitation and emission of 554 and 581 nm, respectively, which are distinct from the autofluorescence range of animal tissues and cells, and permits imaging studies *in vivo* (25–27).

Here, we identified parasites that constitutively expressed the *tdTomato* reporter gene, conferring red fluorescence, and validated a model for screening compounds against *L. (V.) braziliensis* and *L. (L.) infantum*. This model will facilitate high-throughput screens of compounds *in vitro* and *in vivo* and should replace current laborious methodologies that are difficult to reproduce. High-throughput screens of compounds and drugs improve the likelihood that new compounds with activity against *Leishmania* spp. be identified.

RESULTS

Construction of pIR1_BSD_ *tdTomato* plasmids and generation of parasites constitutively expressing *tdTomato*

We amplified the *tdTomato* sequence by PCR then cloned it by Gibson Assembly into the *Bgl*II site of the pIR1_BSD vector to construct the pIR1_BSD_ *tdTomato* plasmid. The plasmids were sequenced using the Sanger method and linearized using the restriction enzyme *Swa*I. Promastigotes of *L. braziliensis* and *L. infantum* were transfected with the cassette and selected in semi-solid medium containing 10 µg/mL of blasticidin (BSD).

Fluorescence emission by parasites transfected with *tdTomato*

We determined whether the promastigote forms of *Lb* wild type (WT), *Lb::tdTomato*, *LlWT*, and *Li::tdTomato* parasites expressed red *tdTomato* fluorescence using flow cytometry. Both mutant parasites expressed red fluorescence (Fig. 1A through C), whereas the WT did not.

We also evaluated the intensity of fluorescence emitted by the mutant parasites. The detection limit of the fluorimeter was $\sim 2 \times 10^3$ parasites/mL for the *Lb::tdTomato* and *Li::tdTomato* promastigotes (Fig. 1D). Fluorescence emission in the intracellular amastigote forms confirmed that *tdTomato* is expressed at different stages of the parasitic life cycle (Fig. 1E). Fluorescence intensity correlated with the number of amastigotes per macrophage (Fig. 1F).

Confocal laser microscopy confirmed that *tdTomato* fluorescence was emitted by *L. braziliensis* mutant and indicated a homogenous distribution throughout in the parasite cytoplasm and flagellum, but no fluorescence was detected on WT promastigotes and amastigotes (Fig. 2).

Fitness evaluation of WT and mutant parasites

Growth curves of the WT (*LbWT*) and mutant (*Lb::tdTomato*) promastigotes were evaluated daily for 7 days (Fig. 3A). Both *Leishmania* lines had the same growth kinetics. They all reached the stationary phase at 4 days and had similar densities (*LbWT* 17.1×10^6 /mL and *Lb::tdTomato* 17.8×10^6 /mL), indicating that the inserted *tdTomato* gene did not affect promastigote replication.

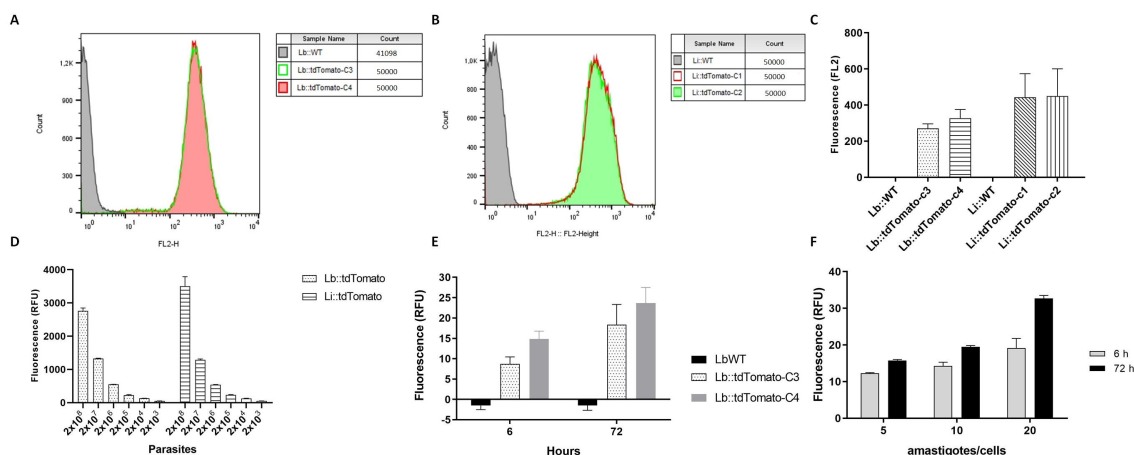


FIG 1 Fluorescence measurement of promastigote and amastigote forms of *Lb::tdTomato* and *Li::tdTomato* mutants. Representative fluorescence histograms in FL2 of promastigotes of WT and cloned mutant parasites *Lb::tdTomato* (A) and *Li::tdTomato* (B). (C) Mean FL2 fluorescence of WT parasites and mutant parasite clones, in arbitrary units obtained in two independent experiments. (D) Fluorescence intensity of various numbers of mutant parasites measured using SpectraMax M2 fluorescence plate reader. (E) Fluorescence emission of WT and two different mutant parasites (*Lb::tdTomato*) after 6 or 72 h after of macrophage infection. (F) Fluorescence emission is proportional to the number of amastigotes per macrophage. Results are representative of two independent experiments in triplicate.

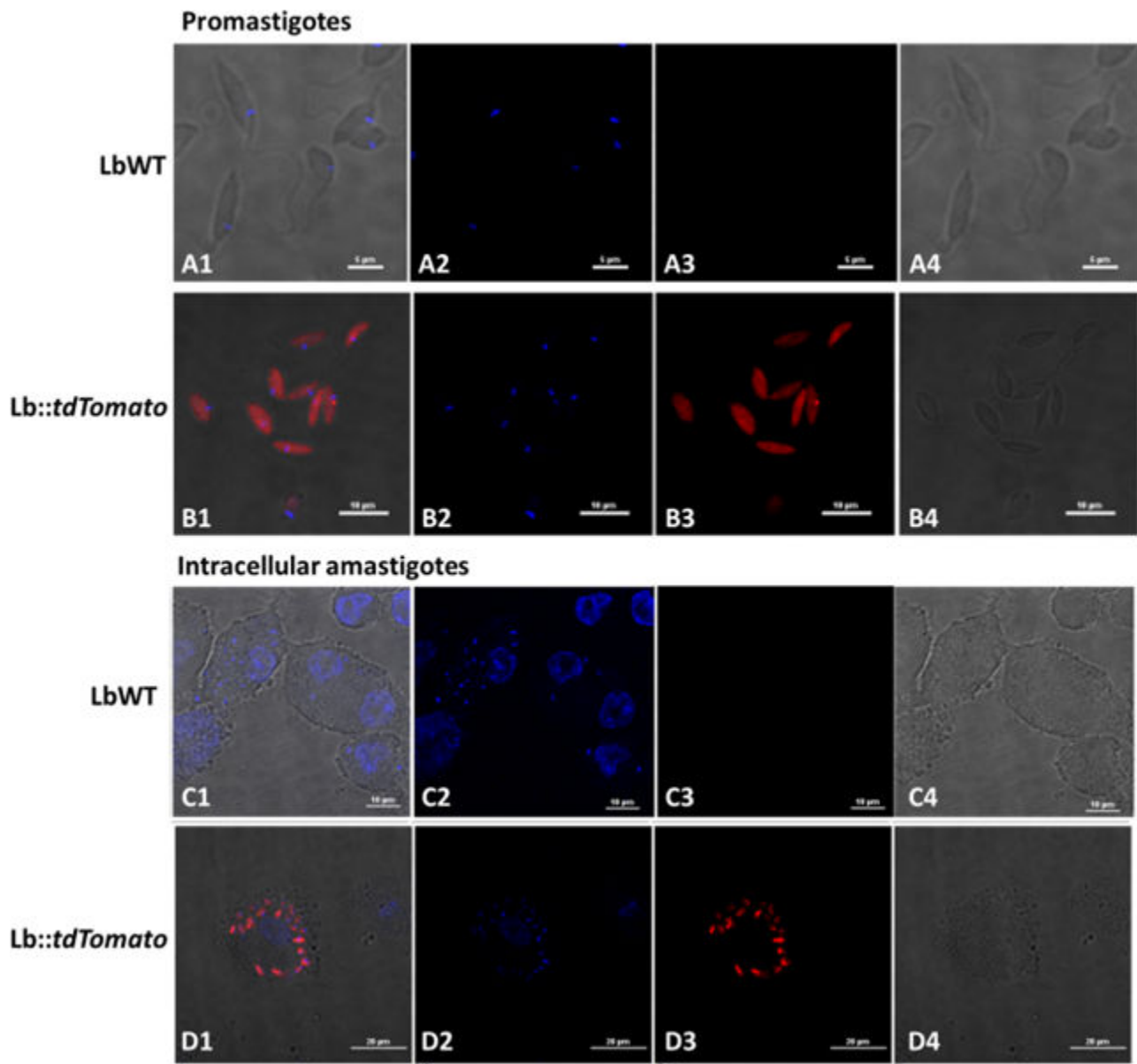


FIG 2 Representative images of promastigotes and intracellular amastigotes of *L. braziliensis* WT or *L. braziliensis* expressing *tdTomato*. (A) Promastigotes of WT *L. braziliensis*. (B) Promastigotes of *L. braziliensis* transfected with *tdTomato*. (C) Amastigotes of WT *L. braziliensis* in THP-1 cells. (D) Amastigote of *L. braziliensis* transfected with *tdTomato* in THP-1 cells. A1, B1, C1, and D1 represent image overlays. A2, B2, C2, and D2 represent DAPI core collation. A3, B3, C3, and D3 represent *tdTomato* fluorescence. A4, B4, C4, and D4 represent differential interference contrast. Images were acquired using confocal laser microscopy at emission and excitation wavelengths of 554 and 581 nm, respectively.

Macrophages derived from THP-1 were infected with WT and mutant parasites to determine whether *tdTomato* expression influences parasite infectivity. Ratios of infected macrophages were determined by counting the number of infected cells and the number of amastigotes per infected cell at 72 h after infection (Fig. 3B and C). We found that *tdTomato* expression did not affect the ability of parasites to infect cells because the infectivity of the WT and mutant *Leishmania* lines was equivalent over the tested post-infection periods.

The anti-*Leishmania* activities of Sb^{III}, miltefosine, and amphotericin B (AmB) were analyzed 72 h after incubation by determining the IC₅₀. We compared conventional and fluorimetric methods by counting the number of amastigotes per macrophage to

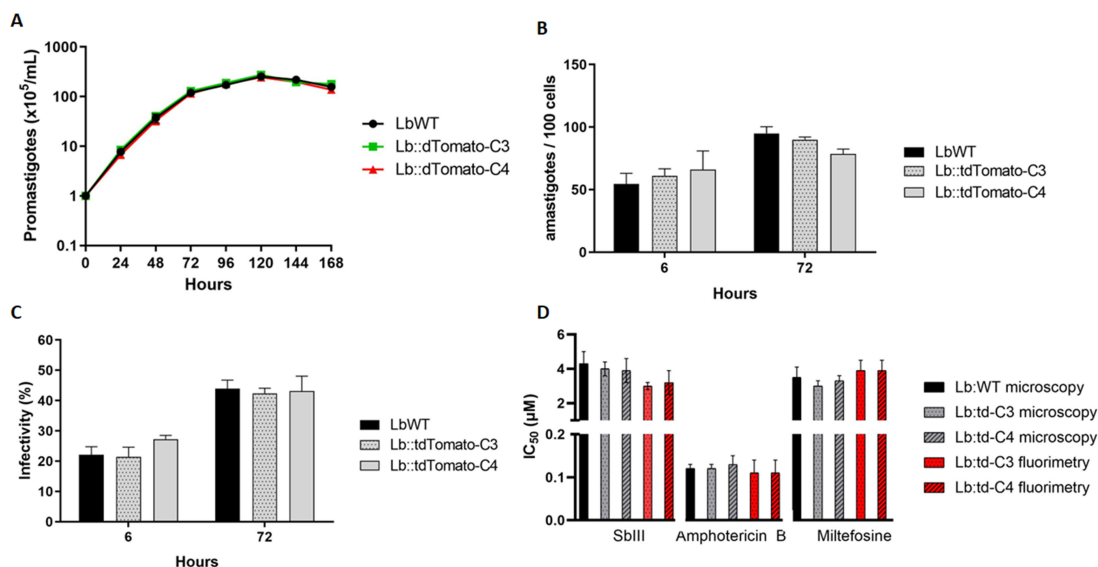


FIG 3 Mutant parasite growth, infectivity, and drug susceptibility are not changed. Growth curves of WT and *Lb::tdTomato* (clones 3 and 4) promastigotes (A). Parasites at 1×10^5 /mL were cultivated for 7 days and counted daily. Data are averages of three independent experiments in triplicate. Curves were statistically analyzed using the two-way analysis of variance with Bonferroni post hoc tests. (B and C) Evaluation of WT and mutant parasites (*Lb::tdTomato*) infectivity in macrophages 6 and 72 h after infection. Infection was evaluated as ratios (%) of the number of amastigotes per 100 macrophages (B) and by the percentage of infected macrophages at 6 and 72 h post infection (C). Results are representative of three independent experiments in duplicate. Anti-*Leishmania* activity of Sb^{III}, miltefosine, and amphotericin B at 72 h after incubation determined as concentration of each drug required to inhibit 50% of parasite growth (IC_{50}) (D). To compare the results of microscopy and fluorimetry, we utilized amastigote counts per macrophage to calculate IC_{50} values. Results represent three independent experiments in duplicate.

determine the IC_{50} . Reductions in these numbers were evaluated as a decrease in the intensity of fluorescence emitted by intracellular amastigotes. We found that the IC_{50} of the drugs tested against WT and mutant *L. braziliensis* amastigotes were very similar between the conventional method and fluorimetry. For the conventional method, the IC_{50} values of Sb^{III}, AmB, and miltefosine were 4.3, 0.12, and 3.5 μ M, respectively. For the fluorimetric method, the IC_{50} values of Sb^{III}, AmB, and miltefosine were 3.2, 0.11, and 3.9 μ M, respectively (Fig. 3D). This finding indicated that integration of the *tdTomato* gene did not affect the susceptibility of mutant parasites to the tested drugs.

Screening substances and extracts

We validated the results of the fluorometric screening as follows. We quantified the IC_{50} values of the reference drugs Sb^{III}, AmB, and miltefosine against the intracellular *L. braziliensis* and *L. infantum* mutant amastigotes and the CC_{50} of these drugs against macrophages derived from THP-1 cells (Table 1). The IC_{50} values against *L. braziliensis* and *L. infantum* mutant parasites were 3.9 and 2.43 μ M for Sb^{III}, 0.13 and 0.25 μ M for AmB, and 3.3 and 3.6 μ M for miltefosine, respectively. The selectivity index (SI) determined based on the ratios of the CC_{50} and IC_{50} values for *Lb* and *Li::tdTomato* was the highest for AmB (2,859 and 1,486). On the other hand, the SI of drugs Sb^{III} and miltefosine was very low for *Lb* and *Li::tdTomato*, 30|48 and 15|14, respectively.

Lb::tdTomato and *Li::tdTomato* infected macrophages were incubated with various concentrations of allopurinol, amitriptyline, isoniazid, lamivudine, menadione, pamidronate, pentamidine, and tamoxifen. The IC_{50} and CC_{50} values were then determined by fluorimetry (Table 1).

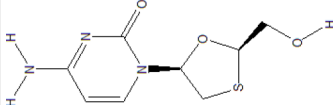
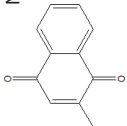
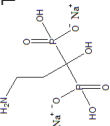
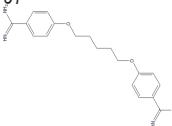
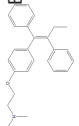
The results showed low antileishmanial activity of amitriptyline and lamivudine, with high IC_{50} values of 106.7 and 2,398 μ M, respectively, for *Lb::tdTomato*, and IC_{50} values of 107.0 and 2,661 μ M, respectively, for *Li::tdTomato*, and a very low SI of 1 (Table 1). The other drugs had IC_{50} values against both leishmania species varied of 0.07 to 10.6 μ M,

TABLE 1 *In vitro* antileishmanial activity (%), inhibitory concentration (IC₅₀) using intracellular amastigote forms of *L. braziliensis* and *L. infantum* transfected with *tdTomato* gene (fluorimetric method), cytotoxicity against THP1 cells (CC₅₀), and SI of reference drugs for clinical treatment and drugs commercially available with the possibility of repositioning for leishmaniasis treatment^a

Drugs	Chemical structure	Clinical indication	Effect on <i>Leishmania</i> spp.	Inhibitory concentration 50%, μM (95% CI)		Selectivity index (SI Lb SI Li) ^d	References
				Amastigotes (IC ₅₀) <i>Lb::tdTomato</i> ^e	Amastigotes (IC ₅₀) <i>Li::tdTomato</i> ^b		
Antimony potassium tartrate (Sb ^{III})		Used for the first time in the trivalent form (SbIII) for the treatment of leishmaniasis.	Glucantime is the drug of first choice for the treatment of leishmaniasis in Brazil	3.90 (3.20–4.60)	2.43 (2.15–2.70)	30 48	(4)
Amphotericin B		Treatment of systemic fungal infections and leishmaniasis	Second-choice therapy, being used in situations of toxicity or therapeutic failure in the treatment with antimony.	0.13 (0.11–0.14)	0.25 (0.22–0.28)	2,859 1,486	(28, 29)
Miltefosine		Developed for the treatment of cutaneous metastases in breast carcinomas	Used in some countries as a second-line treatment for cutaneous leishmaniasis	3.3 (2.6–4.0)	3.6 (3.28–3.95)	15 14	(30, 31)
Allopurinol		Treatment of gouty arthritis (increased serum and urinary levels of uric acid)	Used as drug therapy in the treatment of canine visceral leishmaniasis	3.4 (1.8–4.2)	6.4 (5.3–7.7)	92 49	(32)
Amitriptyline		Depression treatment	Promastigotes and amastigotes of <i>L. amazonensis</i> and <i>L. donovani</i>	106.7 (71.1–227.9)	107.0 (80.9–169.0)	1 1	(33–35)
Isoniazid		Treatment of cases of latent tuberculosis (ILTb)	Promastigotes of <i>L. braziliensis</i> (M2904): IC ₅₀ 7.5 563 μM	7.5 (5.25–9.52)	10.6 (7.6–13.8)	>93 >66	(36)

(Continued on next page)

TABLE 1 *In vitro* antileishmanial activity (%), inhibitory concentration (IC₅₀) using intracellular amastigote forms of *L. braziliensis* and *L. infantum* transfected with *tdTomato* gene (fluorimetric method), cytotoxicity against THP1 cells (CC₅₀), and SI of reference drugs for clinical treatment and drugs commercially available with the possibility of repositioning for leishmaniasis treatment* (Continued)

Drugs	Chemical structure	Clinical indication	Effect on <i>Leishmania</i> spp.	Inhibitory concentration 50%, μM (95% CI)			Selectivity index (SI Lb SI Li) ^d	References
				Amastigotes (IC ₅₀) <i>Lb::tdTomato</i> ^e	Amastigotes (IC ₅₀) <i>Li::tdTomato</i> ^b	Macrophages THP-1 (CC ₅₀) ^c		
Lamivudine		Used in combination with other antiretrovirals to treat human immunodeficiency virus infection.	Promastigotes of <i>L. braziliensis</i> (M2904) IC ₅₀ 766 μM	2,398.0 (1,862.0–3,104.0)	2,661.0 (1,973.0–3,650.0)	2,732.0 (2,032.0–4,030.0)	1 1	(37)
Menadione		Nutritional supplement and in the treatment of hypoprothrombinemia. Important inducer of oxidative stress.	Amastigotes of <i>L. donovani</i> and <i>L. braziliensis</i> . Promastigotes of <i>L. chagasi</i>	8.6 (5.2–13.7)	7.0 (4.6–9.8)	341.0 (195.1–884.7)	40 47	(38)
Pamidronate		Treatment of conditions associated with increased bone-destrory activity; hypercalcemia, bone metastases; osteoporosis.	Promastigotes of <i>L. infantum</i> IC ₅₀ 93.84 μM. Amastigotes of <i>L. infantum</i> IC ₅₀ 1.52 μM	0.6 (0.2–1.1)	1.7 (0.5–2.6)	1,817.0 (1,270.0–3,000.0)	3,028 1,068	(39)
Pentamidine		Second-line drug for the treatment of leishmaniasis.	Second-choice drug for all forms of leishmaniasis (CL, MCL, and VL) unresponsive to antimonial treatment.	5.8 (4.1–8.3)	5.3 (3.6–7.6)	268.1 (133.3–897.4)	46 50	(40, 41)
Tamoxifen		Breast cancer treatment.	Promastigotes and amastigotes of <i>L. braziliensis</i> (IC ₅₀ 1.9 μM) and <i>L. amazonensis</i> ; <i>in vivo</i> assays	0.07 (0.04–0.10)	0.3 (0.2–0.6)	53.2 (40.8–70.9)	760 177	(42, 43)

^aCompound concentration that reduces *Lb::tdTomato* parasite growth by 50% (IC₅₀).

^bCompound concentration that reduces *Li::tdTomato* parasite growth by 50% (IC₅₀).

^cCompound concentration that inhibits 50% the THP-1 cell viability (CC₅₀).

^dThe SI was calculated by the ratio of CC₅₀ THP-1 cells/IC₅₀ *L. braziliensis* or *L. infantum* (SI Lb | SI Li).

^e95% CI, confidence interval 95%; SI, CC₅₀/IC₅₀; μM, micromolar; CL, cutaneous leishmaniasis; MCL, mucocutaneous leishmaniasis; and VL, visceral leishmaniasis.

and the SI range was 40 to 3,028. Pamidronate and tamoxifen were very active against *Leishmania* spp., with IC₅₀ values of 0.6 and 1.7 μM for *L. braziliensis* and 0.07 and 0.3 μM for *L. infantum* and high SI of 3,028|1,068 and 760|177, respectively. In *L. infantum*, these drugs were also very active with IC₅₀ values of 1.7 and 0.3 μM, respectively. Our results revealed that *L. braziliensis* was more susceptible to AmB, allopurinol, isoniazid, pamidronate, and tamoxifen than *L. infantum* (Table 1).

We screened using 32 crude extracts of plants and fungi (20 μg/mL each) and 10 pure substances (50 μM each). The results are expressed as ratios (percentages) of intracellular amastigotes reduced by the crude extracts or pure substances vs untreated controls. Extracts were considered active if their effect against *Leishmania* was higher than 60%. The results showed that 9 of the 32 crude extracts tested were active against the intracellular *Lb::tdTomato* and *Li::tdTomato* amastigotes, and 23 were inactive (Table 2). For the seven extracts with activities higher than 70%, we determined the IC₅₀ and CC₅₀ values. The range of IC₅₀ values of the extracts was 8.1–19.4 μg/mL for *Lb::tdTomato* and 11.2–17.5 μg/mL for *Li::tdTomato*. Most tested extracts had SIs between 2 and 7. The crude extracts of *Clusia mexiae* flowers and of the fungus *Penicillium viridicatum* were the most suitable for future investigations, having IC₅₀ values of 11.4 and 8.9 μg/mL for *Lb::tdTomato* and 17.5 and 13.7 μg/mL for *Li::tdTomato*, respectively (Table 2). SIs of both extracts for *L. braziliensis* and *L. infantum* were 25|16 and 85|55, respectively.

The results showed that 3 of the 10 pure substances were inactive and 7 were active against *L. braziliensis* and *L. infantum* (Table 3). We then determined that the range of IC₅₀ and CC₅₀ values of seven active pure substances was 3.9 to 54.2 μM for *Lb::tdTomato* and *Li::tdTomato*, with an SI range of 8–72. Cinchonine was the most active, with IC₅₀ values of 3.9 and 4.8 μM for *Lb::tdTomato* and *Li::tdTomato* and SIs of 72 and 48, respectively.

Evaluation of infectivity and *in vivo* Glucantime efficacy

We evaluate the infectivity and Glucantime treatment efficacy of animals infected with wild-type and *tdTomato* mutant *L. braziliensis* and *L. infantum* lines.

Hamsters were infected with wild-type and *Lb::tdTomato* *L. braziliensis* lines and treated with Glucantime at 250 mg/kg/day for 20 days. The progress of the lesions was assessed at days 0, 7, 14, 21, and 28. After 7 days of treatment, skin lesions remained similar among groups. Fourteen days after starting treatment, however, the lesions became less thick in the group of hamsters that received Glucantime compared to the untreated group (Fig. 4A). Significant regression of the lesion was observed in animals infected with wild-type and *Lb::tdTomato* parasites after Glucantime treatment (Fig. 4A and D). The results also revealed that Glucantime significantly reduced the parasite loads in the lesions from animals infected with wild-type and *Li::tdTomato* *L. infantum* lines (Fig. 4B). Similar results were obtained with the fluorescence emission (relative fluorescence units - RFU) analysis of *Lb::tdTomato* parasites recovered from lesions (Fig. 4C). Bioimaging assay revealed fluorescence emission in the lesions of hamsters infected with *L. braziliensis* mutant parasites (*Lb::tdTomato*) (Fig. 4E).

Figure 5 shows the parasite burdens in the liver (Fig. 5A) and spleen (Fig. 5B) of BALB/c mice infected with wild-type and *Li::tdTomato* *L. infantum* lines following intraperitoneal administration of the Glucantime at 250 mg/kg/day and 500 mg/kg/day for 10 days. Glucantime at 500 mg significantly reduced the parasite loads in the liver and spleen from animals infected with wild-type and *Li::tdTomato* *L. infantum* lines. Similar results were obtained with the fluorescence emission (RFU) analysis of *Li::tdTomato* parasites recovered from liver and spleen (Fig. 5C).

Our results revealed that the insertion of *tdTomato* gene did not affect infectivity and Glucantime efficacy of animals infected with *Lb::tdTomato* and *Li::tdTomato* lines. The fluorescence emission was efficient to detect infectivity and parasite burdens in the organs and lesions.

TABLE 2 *In vitro* antileishmanial activity (%), inhibitory concentration (IC₅₀), cytotoxicity against THP1 cells (CC₅₀), and SI of extracts against intracellular amastigote forms of *L. braziliensis* and *L. infantum* transfected with *tdTomato* gene (fluorimetric method)^f

Family	Extracts Species	Part	<i>L. braziliensis</i> (<i>Lb::tdTomato</i>)		<i>L. infantum</i> (<i>Li::tdTomato</i>)		CC ₅₀ macrophages THP1 ^d µg/mL (95% CI)	SI ^e (SI Lb SI Li)
			Activity ^a (%)	IC ₅₀ amastigotes ^b µg/mL (95% CI)	Activity ^a (%)	IC ₅₀ amastigotes ^c µg/mL (95% CI)		
Plants								
Asteraceae	<i>Baccharis platypoda</i>	Aerial parts	27.0	Inactive	31.0	Inactive	ND	ND
	<i>B. trinervis</i>	Aerial parts	55.0	Inactive	41.0	Inactive	ND	ND
	<i>Chromolaena laevigata</i>	Aerial parts	46.0	Inactive	58.0	Inactive	ND	ND
	<i>C. squalida</i>	Aerial parts	99.0	9.4 (8.3–10.4)	84.0	15.4 (10.4–22.5)	34.3 (9.1–61.8)	4 2
	<i>Trixis vauthieri</i>	Leaf	91.0	17.8 (12.0–25.3)	83.0	11.2 (6.4–16.2)	128.2 (66.9–399.9)	7 11
	<i>T. vauthieri</i>	Aerial parts	100.0	8.1 (5.9–10.2)	84.0	15.2 (12.1–18.6)	56.5 (34.1–124.6)	7 4
	<i>T. vauthieri</i>	Bough	20.0	Inactive	19.0	Inactive	ND	ND
	<i>T. vauthieri</i>	Aerial parts	25.0	Inactive	33.0	Inactive	ND	ND
	<i>Hololepis pedunculata</i>	Aerial parts	30.0	Inactive	42.0	Inactive	ND	ND
	<i>Aldama robusta</i>	Aerial parts	28.0	Inactive	32.0	Inactive	ND	ND
	<i>Piptocarpha axillares</i>	Leaf	32.0	Inactive	40.0	Inactive	ND	ND
	<i>Baccharis crista</i>	Aerial parts	50.0	Inactive	57.0	Inactive	ND	ND
	<i>Cyrtocymura scorpioides</i>	Leaf	44.0	Inactive	46.0	Inactive	ND	ND
	<i>Trichogonia hirtiflora</i>	Leaf	70.0	19.4 (17.1–22.0)	78.0	14.0 (8.6–20.0)	84.5 (23.0–372.6)	4 6
Annonaceae	<i>Duguetia furfuracea</i>	Fruit	52.0	Inactive	53.0	Inactive	ND	ND
Calophyllaceae	<i>Kielmeyera neriifolia</i>	Leaf	43.0	Inactive	32.0	Inactive	ND	ND
	<i>K. coriacea</i>	Leaf	37.0	Inactive	31.0	Inactive	ND	ND
Cecropiaceae	<i>Cecropia glaziovii</i>	Root	9.0	Inactive	17.0	Inactive	ND	ND
Clusiaceae	<i>Symphonia globulifera</i>	Leaf	11.0	Inactive	25.0	Inactive	ND	ND
	<i>S. globulifera</i>	Bough	18.0	Inactive	30.0	Inactive	ND	ND
	<i>S. globulifera</i>	Flower	26.0	Inactive	31.0	Inactive	ND	ND
	<i>Clusia mexiae</i>	Flower	72.0	11.4 (9.2–13.8)	83.0	17.5 (14.7–20.6)	281.7 (45.0–342.0)	25 16
Myrtaceae	<i>Plinia nana</i>	Leaf	63.0	ND	65.0	ND	ND	ND
	<i>Blepharocalyx salicifolius</i>	Leaf	64.0	ND	67.0	ND	ND	ND
Piperaceae	<i>Peperomia galioides</i>	Aerial parts	34.0	Inactive	29.0	Inactive	ND	ND
Siparunaceae	<i>Siparuna guianensis</i>	Bough	70.0	18.0 (13.0–24.5)	63.0	14.2 (12.3–16.2)	34.8 (21.4–70.3)	2 2
Verbenaceae	<i>Lippia rotundifolia</i>	Aerial parts	42.0	Inactive	38.0	Inactive	ND	ND
Fungi								
Trichocomaceae	<i>Penicillium citrinum</i>	Cultivation, organic phase	35.0	Inactive	50.0	Inactive	ND	ND
	<i>P. corylophilum</i>	Cultivation, organic phase	44.0	Inactive	58.0	Inactive	ND	ND
	<i>P. fellutanum</i>	Cultivation, organic phase	39.0	Inactive	50.0	Inactive	ND	ND
	<i>P. janthinellum</i>	Cultivation, organic phase	41.0	Inactive	49.0	Inactive	ND	ND
	<i>P. viridicatum</i>	Cultivation, organic phase	73.0	8.9 (6.1–11.6)	75.0	13.7 (9.4–18.2)	752.2 (133.0–481.7)	85 55

^aReduction percentage of intracellular amastigote forms (*L. braziliensis tdTomato* and *L. infantum tdTomato*) under the action of the extract.

^bCompound concentration that reduces *Lb::tdTomato* parasite growth by 50% (IC₅₀).

^cCompound concentration that reduces *Li::tdTomato* parasite growth by 50% (IC₅₀).

^dCompound concentration that inhibits 50% the THP-1 cell viability (CC₅₀).

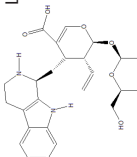
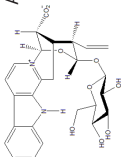
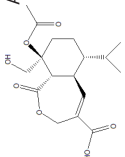
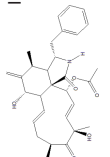
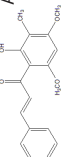
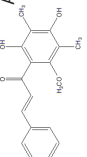
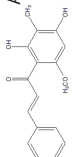
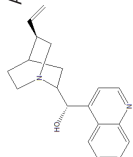
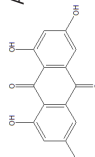
^eThe SI was calculated by the ratio of CC₅₀ THP-1 cells/IC₅₀ *L. braziliensis* or *L. infantum* (SI Lb | SI Li).

^fND, not determined; 95% CI, confidence interval 95%; SI, CC₅₀/IC₅₀; µg/mL, microgram per milliliter; inactive extracts, effect against Leishmania growth lower than 60%.

DISCUSSION

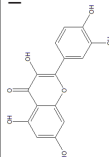
Novel chemotherapeutic strategies and assays are urgently needed to screen new active compounds against *Leishmania*. Several drug screening procedures have been developed to increase the efficacy and reliability of the results compared with classical

TABLE 3 *In vitro* antileishmanial activity (%), inhibitory concentration (IC₅₀), cytotoxicity against THP1 cells (CC₅₀), and SI of pure substances against intracellular amastigote forms of *L. braziliensis* and *L. infantum* transfected with *tdTomato* gene (fluorimetric method)^f

Substances	Origin	Molecular structure	Effect on <i>Leishmania</i> spp.	Activity ^a (%)	IC ₅₀ amastigotes ^b μM (95% CI) <i>Le:tdTomato</i>	IC ₅₀ amastigotes ^c μM (95% CI) <i>CC-50 macrophages THP1^d SI^e</i>	CC ₅₀ μM (95% CI)	References
Strycostodinic acid	<i>Psychotria cupularis</i>		Little active on <i>L. (V.) braziliensis</i> and <i>L. (L.) amazonensis</i>	57	42.4 (29.0–60.0)	8 10	347.0 (257.0–555.0)	(44)
Ophiorine B	<i>Psychotria cupularis</i>		Active against <i>L. (V.) braziliensis</i> (IC ₅₀ 196.1 μM) and <i>L. (L.) amazonensis</i> (IC ₅₀ 7.2 μM)	70	28.60 (20.0–37.0)	14 12	388.4 (280.0–614.0)	(44)
10-Acetyl tricoderonic acid A	<i>Nectria pseudotrichia</i>		Active against intracellular amastigotes of <i>L. (V.) braziliensis</i> (IC ₅₀ 21.4 μM)	57	14.9 (12.0–17.0)	9 10	141.3 (93.6–190.9)	(45)
Cytochalasin D	<i>Nectria pseudotrichia</i>		Inactive against <i>L. (V.) braziliensis</i>	33	Inactive	ND	ND	(45)
Chalcona 1	<i>Blepharocalyx salicifolius</i>		Active against <i>L. (L.) amazonensis</i>	70	19.9 (13.0–26.0)	12 10	238.0 (141.0–319.0)	(46)
Chalcona 2	<i>Blepharocalyx salicifolius</i>		Active against <i>L. (L.) amazonensis</i>	11	Inactive	ND	ND	(46)
Chalcona 3	<i>Blepharocalyx salicifolius</i>		Active against <i>L. (L.) amazonensis</i>	7	Inactive	ND	ND	(46)
Cinchonin	Roth, comercial		Active against promastigotes forms of <i>L. mexicana</i> (IC ₅₀ 4.11 μg/mL)	ND	3.9 (1.6–6.3)	72 58	280.0 (172.7–555.7)	(47)
Emodin	Roth, comercial		Active against promastigotes forms of <i>L. braziliensis</i> (IC ₅₀ 3.20 μg/mL)	ND	52.3 (35.2–95.7)	21 20	1084.0 (648.2–2,983.0)	(48)

(Continued on next page)

TABLE 3 *In vitro* antileishmanial activity (%), inhibitory concentration (IC₅₀), cytotoxicity against THP1 cells (CC₅₀), and SI of pure substances against intracellular amastigote forms of *L. braziliensis* and *L. infantum* transfected with *tdTomato* gene (fluorimetric method)¹ (Continued)

Substances	Origin	Molecular structure	Effect on <i>Leishmania</i> spp.	Activity ^a (%)	IC ₅₀ amastigotes ^b μM (95% CI) <i>Lb::tdTomato</i>	IC ₅₀ amastigotes ^c μM (95% CI) <i>Li::tdTomato</i>	CC ₅₀ macrophages THP1 ^d SI ^e (SI Lb SI Li)	References
Quercetin	Gifted by Simon Croft		It was able to inhibit the growth of amastigotes of <i>L. amazonensis</i> , <i>L. donovani</i> and <i>L. braziliensis</i>	ND (16.3–23.9)	15.08 (12.2–18.1)	802.9 (349.3–1,024.0)	40 53 (49, 50)	
Amphotericin B	-	-	-	ND (0.11–0.14)	0.25 (0.22–0.28)	371.7 (309–446)	2,859 1,487	

^aReduction percentage of intracellular amastigote forms (*L. braziliensis tdTomato* and *L. infantum tdTomato*) under the action of the substance.

^bCompound concentration that reduces *Lb::tdTomato* parasite growth by 50% (IC₅₀).

^cCompound concentration that reduces *Li::tdTomato* parasite growth by 50% (IC₅₀).

^dCompound concentration that inhibits 50% the THP-1 cell viability (CC₅₀).

^eThe SI was calculated by the ratio of CC₅₀ THP-1 cells/IC₅₀ *L. braziliensis* or *L. infantum* (SI Lb | SI Li).

^fND, not determined; 95% CI, confidence interval 95%; SI, CC₅₀/IC₅₀; inactive extracts, effect against *Leishmania* growth lower than 50%.

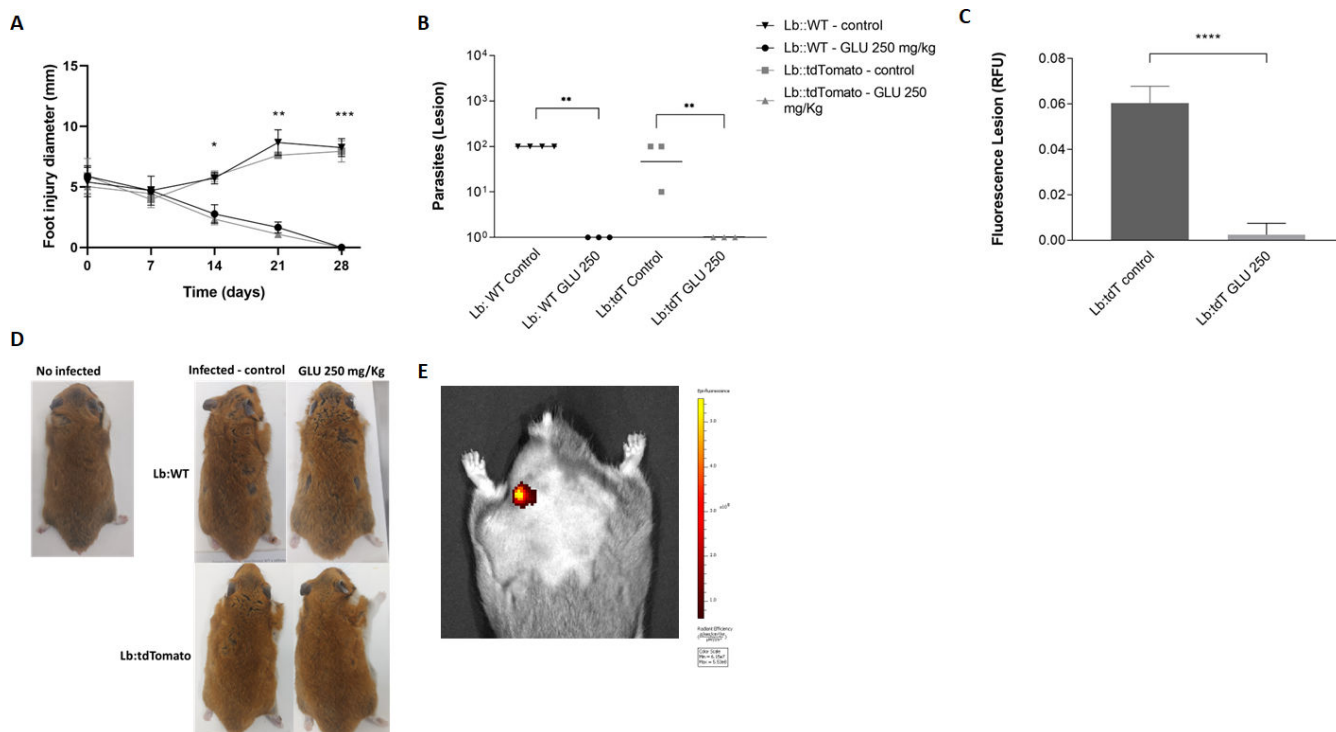


FIG 4 Evaluation of infectivity and *in vivo* Glucantime efficacy of golden hamsters infected with wild-type and *tdTomato* mutant *L. braziliensis* lines. Animals were treated intramuscular route with Glucantime at 250 mg/kg/day for 20 days. Vertical bars represent the average and standard error of lesion size (diameter) (A). The treatment was evaluated through the number of parasites recovered from the lesions comparing animals treated and not treated with Glucantime. The horizontal bars represent the average number of viable parasites in the lesions for each group (B). We evaluated the fluorescence emission of recovered parasites from lesions (RFU) (C). Images comparing hamsters infected with wild-type (*Lb:WT*) and mutants (*Lb:tdTomato*) parasites untreated and treated with GLU (D). Bioimaging assay of infection in golden hamsters with *L. braziliensis tdTomato* parasites at the base of tail (E). One-way analysis of variance with Bonferroni post hoc test was used to compare the treated groups in relation to the control group without treatment. Asterisk (*) represents significant differences in relation to the control group without treatment (* $P < 0.05$, ** $P < 0.01$, *** $P < 0.001$, and **** $P < 0.0001$). Control: infected and untreated animals. GLU 250: animals infected and treated with 250 mg/kg of Glucantime.

methodologies. Green fluorescent protein, bioluminescent (luciferase), RFP, and colorimetric (chloramphenicol, acetyl transferase, β -galactosidase, and alkaline phosphatase) reporter genes are currently applied to screen compounds with anti-*Leishmania* activity *in vitro* (12–16, 20–23, 51–53). However, these methodologies have some disadvantages for screening compounds with anti-*Leishmania* activity *in vivo* and *in vitro*, such as requiring an added substrate for luminescence detection. This increases screening costs, and exogenous substrate interaction with compounds during colorimetric tests can generate incorrect results (6). Here, we validated *L. braziliensis* and *L. infantum* that constitutively express the tandem tomato RFP *tdTomato* as a model for large-scale screens of anti-*Leishmania* compounds.

The RFP *tdTomato* can be used to screen drugs against trypanosomatids *in vitro* and *in vivo* (25–27). We similarly found that expressing *tdTomato* does not affect the fitness of parasites in terms of growth, infectivity, and drug susceptibility.

Leishmania intracellular amastigotes comprise the main target of searches for new drugs and compounds for treating leishmaniasis, since it is the parasite form that replicates within macrophages in the vertebrate host (54, 55). Since promastigotes and amastigotes present several metabolic differences, by screening compounds against *Leishmania* intracellular amastigotes, we can find hits specific to the parasite form capable of infecting and persisting in host cells (54–56). Here, we infected macrophages derived from THP-1 cells with WT and mutant *L. braziliensis* and *L. infantum* parasites and then analyzed red fluorescence emission using confocal microscopy, flow cytometry, and fluorometry. We confirmed that fluorescence persisted in intracellular amastigotes, thus

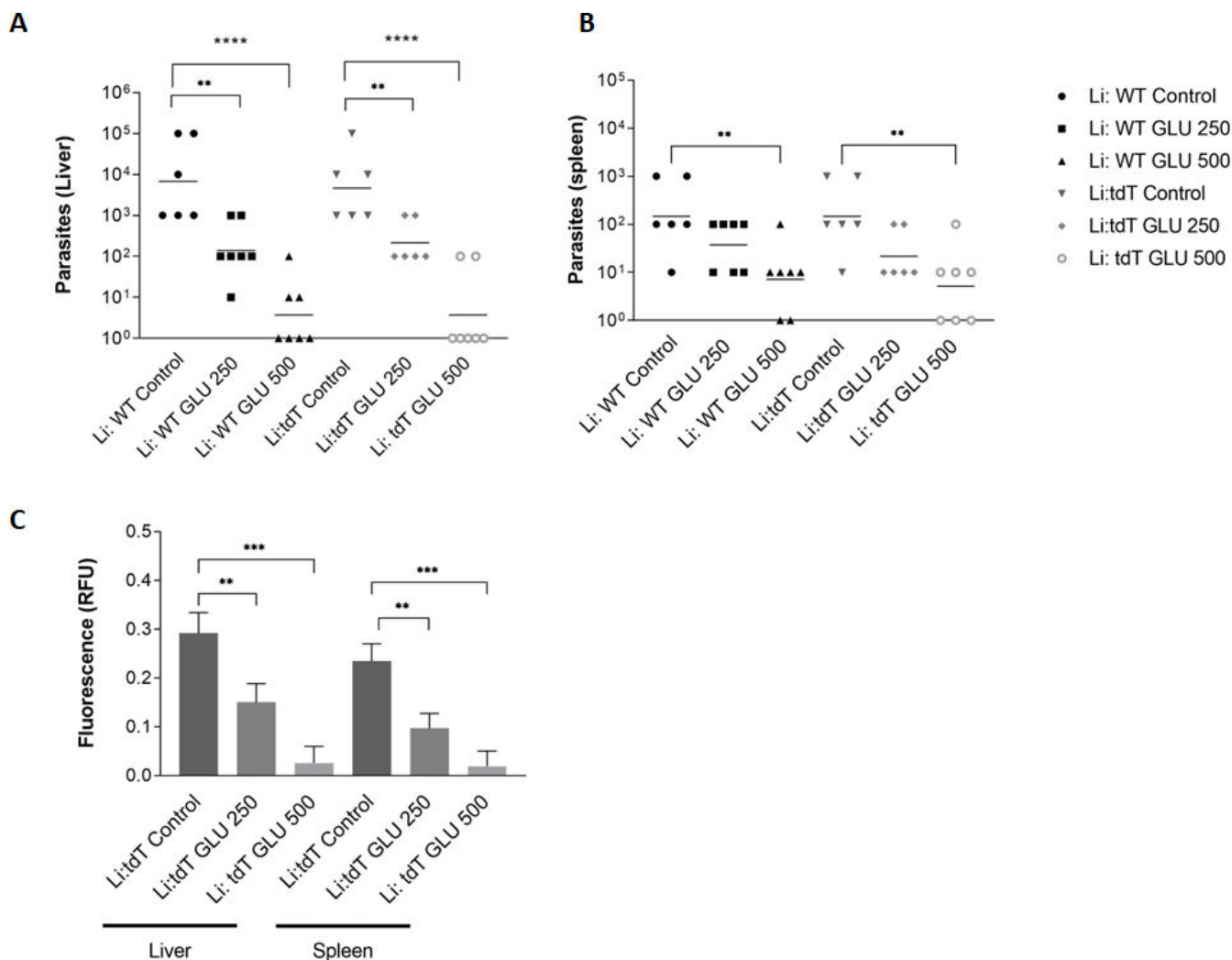


FIG 5 Evaluation of infectivity and *in vivo* Glucantime efficacy of BALB/c mice infected with wild-type and *tdTomato* mutant *L. infantum* lines. Animals infected were treated by intraperitoneal administration of the Glucantime at 250 mg/kg/day and 500 mg/kg/day for 10 days. The treatment was evaluated through the number of parasites recovered from the liver (A) and spleen (B) of animals treated and not treated with Glucantime. The horizontal bars represent the average number of viable parasites in the liver and spleen for each group. The fluorescence emission (RFU) of parasites recovered from liver and spleen (C). One-way analysis of variance with Bonferroni post hoc test was used to compare the treated groups in relation to the control group without treatment. Asterisk (*) represents significant differences in relation to group without treatment (** $P < 0.01$, *** $P < 0.001$, and **** $P < 0.0001$). Control: infected and untreated animals. GLU 250 and GLU 500: animals infected and treated with 250 or 500 mg/kg of Glucantime, respectively.

supporting the notion that our semi-automated model can be applied to screening anti-*Leishmania* compounds. Our conventional and fluorometric evaluation of intracellular amastigote susceptibility to Sb^{III} (4), AmB (28, 29), and miltefosine (30, 31) revealed a very close correlation between the two methods.

We applied our validated model to a repositioning strategy and assessed the susceptibility of the parasites to eight commercially available drugs: allopurinol (32), amitriptyline (33–35), isoniazid (36), lamivudine (37), menadione (38), pamidronate (39), pentamidine (40, 41), and tamoxifen (42, 43) (Table 1).

Pamidronate used to treat cancer also showed anti-*Leishmania* and immunomodulatory potential against *L. infantum* *in vitro* and *in vivo* (39). We found that pamidronate was very active against intracellular amastigotes expressing *tdTomato*. The IC₅₀ value of this drug was 1.7 μ M for *Li:tdTomato*, similar to that described in the literature (1.527 μ M) (39) and 0.6 μ M for *Lb:tdTomato*, and its low toxicity to mammalian cells, with SI of 3,028 and 1,068, rendered it suitable for assays *in vivo*.

Tamoxifen is used to treat breast cancer because it modulates estrogen receptor activity (42). This compound has activity *in vivo* against *L. (L.) amazonensis* and *L. (V.) braziliensis* that cause cutaneous leishmaniasis and *L. (L.) chagasi* that is responsible for visceral leishmaniasis (42, 43). Here, the tamoxifen was extremely active against *L. braziliensis* and *L. infantum* transfected with the *tdTomato* reporter gene, showing IC₅₀ values of 0.07 and 0.3 μM, respectively (Table 1). The SI of 760 and 177 showed that tamoxifen was highly selective for mammalian cells. Despite the good SI found in our study, tamoxifen and its metabolites have the ability to interact with a wide range of off-target receptors in the body and are thus possibly associated with a number of negative side effects such as retinal toxicities, cardiovascular events, and endometrial cancer (57, 58).

Allopurinol inhibited purine metabolism and *Leishmania* growth *in vitro*. This oral drug can control relapse of canine leishmaniasis with a very low incidence of side effects (32). This drug was highly selective (SI = 92 and 49) and acted against *L. braziliensis* and *L. infantum* with a low IC₅₀ of 3.4 and 6.4 μM, which was also suitable for further investigation *in vivo*. The same was true for pentamidine, with IC₅₀ values of 5.8 and 5.3 μM and SI of 46 and 50 for *L. braziliensis* and *L. infantum*, respectively. This drug has been administered to fight fungal and protozoan infections (leishmaniasis and African trypanosomiasis) when treatment with Glucantime fails. This compound binds to DNA and inhibits the replication of *Leishmania*, *Pneumocystis carinii*, and *Trypanosoma* (32).

Amitriptyline is a tricyclic antidepressant with sedative effects that inhibit the membrane transport mechanism responsible for the uptake of norepinephrine and serotonin by adrenergic and serotonin neurons (33, 34). It acts against fungi, *T. cruzi*, and *Leishmania* spp. Tricyclic compounds are potential anti-*Leishmania* agents (35). The authors found that amitriptyline acts *in vitro* by reducing proline transport and depleting ATP in *L. (L.) donovani* promastigotes. Others have also found that tricyclic compounds including amitriptyline have anti-*Leishmania* activity in intracellular amastigotes of *L. (L.) amazonensis* and *L. (L.) donovani* (35). The present findings showed that amitriptyline was weakly active, with an IC₅₀ of 107 μM for *L. braziliensis* and *L. infantum*, and the SI of 1 indicated high toxicity to mammalian cells.

Natural products and crude plant and fungal extracts have historically been used to identify substances active against different pathogens (59). Some natural compounds exhibit autofluorescence that overlaps with the *tdTomato* emission spectrum (26, 56); however, none of the drugs or crude extracts tested herein emitted autofluorescence that was close to that of *tdTomato*. Among 32 crude extracts of plants and fungi provided by the “Química de Produtos Naturais Bioativos” at Instituto René Rachou (QPNB/IRR), we extracted 27 from plants belonging to the families *Asteraceae*, *Annonaceae*, *Calophyllaceae*, *Cecropiaceae*, *Myrtaceae*, *Piperaceae*, *Siparunaceae*, and *Verbenaceae* and five from fungal species of the *Trichocomaceae* family (Table 2). We found that extracts of *Asteraceae*, *Annonaceae*, *Clusiaceae*, *Myrtaceae*, *Siparunaceae*, and *Trichocomaceae* acted against *Lb::tdTomato* and *Li::tdTomato*. The IC₅₀ values varied from 8.1 to 19.4 μg/mL, the CC₅₀ from 34.3 to 752.2 μg/mL, and the SI varied between 2 and 85, and most of these extracts were not very selective, such as *Siparuna guianensis*, *Trichogonia hirtiflora*, and *C. squalida*. On the other hand, a flower extract of *Clusia mexiae* belonging to the family *Clusiaceae* was active against *L. braziliensis* and *L. infantum*, with an IC₅₀ of 11.4 and 17.5 μg/mL, and had an SI of 25 and 16. Another active extract from the fungus *Penicillium viridicatum*, belonging to the *Trichocomaceae* family, had an IC₅₀ of 8.9 and 13.7 μg/mL and an SI of 85 and 55. This extract also has herbicidal activity (59).

Because the extracts comprise mixtures of substances, SI values alone cannot be used to decide whether further studies should proceed, since a substance with anti-*Leishmania* activity in extracts might not be the same and could be cytotoxic. Therefore, these substances should be isolated to define their activity and cytotoxicity and confirm the present findings. Therefore, we used the IC₅₀ values to interpret the results and design future studies.

Seven of the 10 pure substances tested herein (Table 3) have been characterized at the QPNB/IRR as ophiorine B (44); strychnosidinic acid (44); 10-acetyl trichoderonic acid A (45); cytochalasin D (45); and chalcones 1, 2, and 3 (46). Three substances were identified as cinchonine: an alkaloid found in *Cinchona officinalis* (47), emodin derived from the endocytic fungus *Penicillium herquei* (48) (both from Carl Roth GmbH + Co. KG, Karlsruhe Germany) as well as quercetin (49, 50) (kindly provided by Dr. Simon L. Croft). Among 10 pure substances tested, seven were active against *L. braziliensis* and *L. infantum* with IC₅₀ values of 3.9 to 54.2 μM and SIs of 8–72, respectively. Pure cinchonine was the most active for *Lb::tdTomato* and *Li::tdTomato* parasites with IC₅₀ values of 3.9 and 4.8 μM and presented SIs of 72 and 58, respectively. Cinchonine, emodin, and quercetin were already tested against *Leishmania*, and it was reported that the IC₅₀ of cinchonine against *L. mexicana* promastigotes is 4.11 μg/mL (13.9 μM) (47), whereas the IC₅₀ of emodin against *L. braziliensis* promastigote is 320 μg/mL (1,184.1 μM) (48). Quercetin has also been demonstrated to prevent the growth of *L. amazonensis* (49) and *L. braziliensis* amastigotes (50). Here, we demonstrated that quercetin reduced *L. braziliensis* and *L. infantum* infection in macrophages derived from THP-1 cells, with an IC₅₀ of 19.2 and 15 μM and SI of 40 and 53, respectively. Quercetin is a bioactive flavonoid found in a variety of fruits, flowers, vegetables, and teas that has antioxidant, anti-inflammatory, antibacterial, and antiparasitic properties (49, 50).

Screening substances *in vivo* is essential for preclinical tests of treatment effects and cytotoxicity, but many animals must be assessed, which is laborious and costly. However, equipment such as the spectrum *in vivo* imaging system (IVIS) offers an excellent alternative for reducing the number of animals and the costs of these evaluations (26, 27). Considering this, we evaluated the infectivity of WT and strains transfected with the *tdTomato* gene in *L. braziliensis* and *L. infantum*. The animals infected with the WT and mutant parasites did not significantly differ, and treatment with Glucantime responded similarly in both lines. This finding opens perspectives on the semi-automation of techniques for screening active compounds *in vitro* and *in vivo* in *L. (V.) braziliensis* and *L. (L.) infantum*, which are *Leishmania* species of significant epidemiological importance in Brazil. This will allow greater efficiency in the identification of active compounds/drugs and pave the way to collaborations with domestic and international research groups (6, 12). We hope to identify oral compounds and drugs that are less toxic and have fewer side effects, which could help to control diseases caused by protozoa of the genus *Leishmania* spp.

In conclusion, *L. braziliensis* and *L. infantum* expressing *tdTomato* can screen anti-*Leishmania* compounds, enabling efficient, cost-effective screening for leishmaniasis treatment.

MATERIALS AND METHODS

Cultivation and maintenance of parasites

Promastigote forms of *Leishmania (Viannia) braziliensis* (MHOM/BR/75/M2903) and *Leishmania (Leishmania) infantum* (MHOM/BR/1974/PP75), originally obtained from the IRR/Fiocruz Minas. The parasites were cultivated in GIBCO M199 medium (Gibco Laboratories, Gaithersburg, MD, USA) supplemented with 10% fetal bovine serum, 5 μg/mL of hemin, and 5 μM of bioperin (pH 7.0) at 26°C. Parasite numbers were determined using a Z1 Coulter Particle Counter (Beckman Coulter, Inc., Brea, CA, USA), and cultures were maintained by two weekly passages, inoculating 1 × 10⁶ parasites/5 mL of medium.

Construction of plasmid pIR1_BSD_tdTomato

The coding sequence of *tdTomato* was amplified by PCR using Phusion high-fidelity Taq DNA polymerase [New England Biolabs, Inc. (NEB), Ipswich, MA, USA) and the plasmid pcDNA3.1(+)/Luc2=tdT (catalog no. 32904; Addgene, Watertown, MA, USA) as the DNA template (60). Primers for amplifying a *tdTomato* fragment compatible with the Gibson

Assembly reaction were designed as follows using the NEBuilder Assembly Tool (<http://nebuilder.neb.com/>): tdTomato_F: CCTCGCTGCCCGCTCCGGACCACCATGGTGAGCAAGG
tdTomato_R: AGTACATCACAACTCATATTACTTGTACAGCTCGTC.

The PCR product was cloned into the pIR1_BSD vector using a Gibson Assembly Cloning Kit (NEB) as described by the manufacturer. Plasmids were transformed by heat shock into calcium-competent *Escherichia coli* DH5-alpha and purified using EZNA Plasmid DNA Mini Kits (Omega Bio-Tek, Inc., Norcross, GA, USA).

Sanger sequencing

We sequenced the construct using the Sanger method (GeneWiz). Contigs were assembled using DNASTAR software, and sequences were analyzed using MultAlin software (<http://multalin.toulouse.inra.fr/multalin/>).

Transfection

The pIR1_BSD_tdTomato plasmid was linearized upon *Swa*I digestion, and the wild-type *Leishmania* spp. were transfected by electroporation as previously described (60). This construct integrates into the 18S ribosomal DNA small subunit locus by homologous recombination (61). Parasites were selected in a semi-solid M199 medium containing 1% agar and 10 µg/mL of BSD (Gibco Laboratories).

Drugs, crude extracts, and pure substances

We purchased drugs from the following sources: AmB (Laboratorios Richet, Buenos Aires, Argentina); miltefosine and tamoxifen (Cayman Chemical, Ann Arbor, MI, USA); antimony tartrate Sb^{III}, menadione, and pamidronate (Sigma-Aldrich Corp., St. Louis, MO, USA); isoniazid (Farmanguinhos/Fiocruz, Rio de Janeiro, Brazil); lamivudine (Globe Química, Cosmópolis, Brazil); allopurinol (Pharma Roth GmbH, Wiesbaden, Germany); and amitriptyline and pentamidine (kindly provided by Dr. Simon Croft, London School of Hygiene and Tropical Medicine, London, UK).

The research group QPNB/IRR has a library of ~20,000 crude extracts isolated from plants and fungi. Samples of plants (~200 mg) were placed in Falcon-type tubes and extracted with ethanol in the field. Fungi were cultivated in culture medium and extracted in ethyl acetate. The solvents were removed by vacuum centrifugation, and then, crude extracts (20 mg/mL) were stored in aqueous DMSO at -20°C.

Furthermore, 32 crude plant and fungal extracts of natural products and 10 pure substances provided by QPNB/IRR were screened for antileishmanial activity against intracellular amastigote forms of *Lb::tdTomato* and *Li::tdTomato*. The concentrations of extracts and pure substances for initial screening were 20 µg/mL and 50 µM, respectively.

Parasite growth curves

WT and mutant *L. braziliensis* and *L. infantum* were inoculated into M199 at an initial concentration of 1×10^5 parasites/mL. Growth over 7 days was determined daily using a Z1 Coulter Particle Counter (Beckman Coulter).

Cultivation, maintenance, and infection of THP-1 cells

Monocytes derived from the THP-1 human monocytic lineage (available in our laboratory sample collection) were cultured in complete RPMI 1640 medium (Gibco) supplemented with 10% fetal bovine serum, 2 mM glutamine, 100 U/mL penicillin, and 100 µg/mL streptomycin. Cultures were maintained by two weekly passages inoculated with 5×10^5 cells/25 mL of medium. The THP-1 cells were differentiated into macrophages by adding phorbol myristate acetate (20 ng/mL) to the cultures. We assayed infectivity by incubating 4×10^5 or 5×10^4 macrophages/well (as indicated) to 24-well plates and 4×10^5 /well to 96-well plates for 72 h. Thereafter, the macrophages were infected with WT and mutant promastigotes of *L. braziliensis* (5, 10, or 20/macrophage, as indicated) at the

stationary phase for 4 h. Parasites that did not infect the macrophages were eliminated by several washes. Intracellular amastigote development was evaluated at 6 and 72 h of incubation, either by staining coverslips with Rapid Panotic (Laborclin, São José do Rio Preto, Brazil) or using black, clear-bottomed Costar 96-well plates (Corning, Inc., Corning, NY, USA) and a SpectraMax M5 fluorescence plate reader (Molecular Devices LLC, Sunnyvale, CA, USA).

Flow cytometry

Mutant and WT promastigotes were evaluated using a FACSCalibur flow cytometer (Becton Dickinson, Mountain View, CA, USA). We acquired 50,000 events per sample, and data were analyzed using FlowJo v10 (BD Biosciences, San Jose, CA, USA).

Confocal laser microscopy

Promastigote forms of WT and mutant THP-1 cells were fixed in 4% formaldehyde-PBS and then mounted using ProLong Gold Antifade Mountant with DNA stain DAPI (Invitrogen, Carlsbad, CA, USA). Images were acquired using a Nikon C2+ confocal microscope (Nikon Instruments, Inc., Tokyo, Japan) at the IRR.

Susceptibility assays of promastigotes *in vitro*

Mutant and WT *L. braziliensis* and *L. infantum* promastigotes (1×10^6 /mL) were incubated with various concentrations of drugs or extracts at 26°C for 48 h. Parasite growth with and without drugs was determined as optical density at 600 nm or by measuring fluorescence in black, clear-bottomed Costar 96-well plates (Corning, Inc.) using the SpectraMax M2 plate reader. The concentration required to inhibit 50% of the growth (IC₅₀) was determined by the non-linear regression-variable slope model per the equation, log (inhibitor) vs response in GraphPad Prism v.8.2.0 (GraphPad Software, Inc., San Diego, CA, USA).

Susceptibility assays of amastigotes *in vitro*

After infection as described above, THP-1 macrophages were incubated in RPMI medium with increasing concentrations of trivalent antimony (Sb^{III}), AmB, and miltefosine. The IC₅₀ was evaluated using coverslips stained with Rapid Panotic (Laborclin) or by assessing decreases in parasite fluorescence emission with or without the drug after incubation for 72 h. The IC₅₀ of drugs was determined using the non-linear regression-variable slope model per the equation, log (inhibitor) vs response in GraphPad Prism v.8.2.0 (GraphPad Software, Inc.) The results are expressed as ratios (percentages) of effectiveness of the extracts and pure substances compared with untreated controls.

Cytotoxicity in macrophages derived from THP-1 cells

We evaluated cytotoxicity by incubating non-infected and infected macrophages derived from THP-1 cells with drugs for 72 h at 37°C under a 5% CO₂ atmosphere. Cell viability was assessed by staining with Alamar Blue (Invitrogen) (62) for 4 h, and then, absorbance was measured at 570 and 600 nm. The results are expressed as the concentration of each drug required to kill 50% of the cells (CC₅₀) compared with untreated control cells and were calculated by nonlinear regression using GraphPad Prism 8.0 (GraphPad Software, Inc.)

The SI was calculated as the ratio of the cytotoxicity (CC₅₀) of the compounds in macrophages to the activity (IC₅₀) against intracellular amastigotes of *Leishmania* spp.

Infection and treatment of animals

The animals were handled according to the protocols approved by the Ethical Committee for Animal Experimentation of the IRR/Fiocruz Minas (license no. LW-7/23). They were

obtained from the Centro de Bioterismo of IRR/Fiocruz Minas. Free access to a standard diet was allowed, and tap water was supplied *ad libitum*.

Golden hamsters (*Mesocricetus auratus*) (male, 100 to 110 g) were infected by subcutaneous injection in the hind footpad with 1×10^7 late-log-phase promastigotes from wild-type and *Lb::tdTomato L. braziliensis* lines. After 20 days of infection, hamsters (four per group) were treated for 20 consecutive days with meglumine antimoniate (Glucantime, Sanofi Medley Farmacêutica, Suzano, SP, Brazil) given by intramuscular injection at 250 mg/kg/day. The lesions were examined weekly for 4 weeks by measuring the size of the infected footpad with a vernier caliper. The animals were euthanized 30 days after the end of the treatment, and the fragments from cutaneous lesions were isolated from each animal.

BALB/c mice (male, 6 to 8 weeks old, 18 to 20 g) were inoculated intravenously (via tail vein) with 2×10^7 late-log-phase promastigotes from wild-type and *Li::tdTomato L. infantum* lines. After 7 days of infection, mice (six per group) were treated for 10 consecutive days with meglumine antimoniate (Glucantime, Sanofi Medley) given by the intraperitoneal route at 250 mg/kg/day and 500 mg/kg/day. Mice were euthanized 3 days after the end of the treatment, and the liver and spleen were collected from each animal.

The numbers of viable parasites in the liver, spleen, and fragments from cutaneous lesions of animals were determined using the quantitative limiting dilution assay. Briefly, organs and fragments were macerated using an Ultra-Turrax disperser (IKA-Werke GmbH & Co. KG, Staufen, Germany), and a tissue homogenate was obtained with 1 mL of M199 medium. Each tissue homogenate was serially diluted (10-fold) into in 96-well flat-bottom microtiter black plates and incubated at 26°C for 10 days. The wells containing motile promastigotes were identified with an inverted microscope (Axiovert 25; Zeiss), and the parasite burden was determined from the highest dilution at which promastigotes had grown after 10 days of incubation. The parasite load was also determined by fluorimetry using the SpectraMax M2 microplate reader at 554 and 581 nm, respectively. The hamsters were placed ventrally in the IVIS Spectrum *in vivo* imaging system (PerkinElmer, Inc., Waltham, MA, USA), and fluorescence was assessed at 554 and 581 nm, respectively.

Statistical analyses

Data were statistically analyzed using GraphPad Prism 8 (GraphPad Software, Inc.). The normality of the data was tested. Data with parametric distributions were assessed using analysis of variance tests, followed by Bonferroni post hoc tests. Values with $P < 0.05$ were considered significantly different.

ACKNOWLEDGMENTS

We thank the Graduate Program in Health Science (Institute René Rachou - IRR/FIOCRUZ) for its support and the Program for Technological Development in Tools for Health-PDTIS-Fiocruz for the use of its facilities at the IRR/FIOCRUZ. The authors also thank Dr. Stephen Beverley for kindly providing the pIR1-BSD expression vector, and Dr. Simon Croft and Dr. Kátia F Rodrigues for kindly providing some compounds and the fungi samples, respectively. We would like to thank Editage (<https://www.editage.com/>) for English language editing. Our special thanks to two anonymous reviewers that contributed significantly to the revision and improvement of this manuscript.

This investigation received financial support from the following agencies: Fundação de Amparo à Pesquisa do Estado de Minas Gerais (FAPEMIG: APQ-02816-21, APQ-00757-21, BPD-00657-22, RED-00104-22), Convênio Fiocruz-Institut Pasteur-USP (no grant number), Programa INOVA FIOCRUZ - Fundação Oswaldo Cruz (VPPCB-007-FIO-18-2-94), Conselho Nacional de Desenvolvimento Científico e Tecnológico (CNPq 304158/2019-4), and Coordenação de Aperfeiçoamento de Pessoal de Nível Superior - Brasil (CAPES) - Finance Code 001. E.O., T.M.A., and S.M.F.M. are CNPq research fellows. M.G.F.M.L.C. and A.M.M.S. are supported by CAPES.

All authors listed made substantial, direct, and intellectual contributions to the work and read and approved the final manuscript for publication.

We declare that the research was conducted in the absence of any commercial or financial relationships that could be construed as a potential conflict of interest.

AUTHOR AFFILIATIONS

¹Genômica Funcional de Parasitos, Instituto René Rachou, Fundação Oswaldo Cruz FIOCRUZ Minas, Belo Horizonte, Minas Gerais, Brazil

²Química de Produtos Naturais Bioativos, Instituto René Rachou, Fundação Oswaldo Cruz FIOCRUZ Minas, Belo Horizonte, Minas Gerais, Brazil

³Pesquisa Clínica e Políticas Públicas em Doenças Infecto-Parasitárias, Instituto René Rachou, Fundação Oswaldo Cruz FIOCRUZ Minas, Belo Horizonte, Minas Gerais, Brazil

AUTHOR ORCIDs

Mariza Gabriela Faleiro de Moura Lodi Cruz  <http://orcid.org/0000-0003-0828-790X>

Ana Maria Murta Santi  <http://orcid.org/0000-0002-9791-6554>

Edward Oliveira  <http://orcid.org/0000-0002-0042-5178>

Tânia Maria de Almeida Alves  <http://orcid.org/0000-0002-0582-3968>

Silvane Maria Fonseca Murta  <http://orcid.org/0000-0002-8523-2155>

FUNDING

Funder	Grant(s)	Author(s)
Fundação Oswaldo Cruz (FIOCRUZ)	Programa INOVA FIOCRUZ - VPPCB-007-FIO-18-2-94	Silvane Maria Fonseca Murta
Fundação de Amparo à Pesquisa do Estado de Minas Gerais (FAPEMIG)	APQ 02816-21, BPD-00657-22, RED-00104-22, APQ-00757-21	Silvane Maria Fonseca Murta Tânia Maria de Almeida Alves
Conselho Nacional de Desenvolvimento Científico e Tecnológico (CNPq)	CNPq 304158/2019-4	Silvane Maria Fonseca Murta
Coordenação de Aperfeiçoamento de Pessoal de Nível Superior (CAPES)	Finance Code 001	Mariza Gabriela Faleiro de Moura Lodi Cruz Ana Maria Murta Santi

REFERENCES

- World health organization. 2023. Leishmaniasis. Retrieved 19 Aug 2023. <https://www.who.int/news-room/fact-sheets/detail/leishmaniasis>.
- Burza S, Croft SL, Boelaert M. 2018. Leishmaniasis. *The Lancet* 392:951–970. [https://doi.org/10.1016/S0140-6736\(18\)31204-2](https://doi.org/10.1016/S0140-6736(18)31204-2)
- Pace D. 2014. Leishmaniasis. *J Infect* 69 Suppl 1:S10–8. <https://doi.org/10.1016/j.jinf.2014.07.016>
- Muraca G, Berti IR, Sbaraglini ML, Fávoro WJ, Durán N, Castro GR, Talevi A. 2020. Trypanosomatid-caused conditions: state of the art of therapeutics and potential applications of lipid-based nanocarriers. *Front Chem* 8:601151. <https://doi.org/10.3389/fchem.2020.601151>
- Murray HW, Berman JD, Davies CR, Saravia NG. 2005. Advances in leishmaniasis. *The Lancet* 366:1561–1577. [https://doi.org/10.1016/S0140-6736\(05\)67629-5](https://doi.org/10.1016/S0140-6736(05)67629-5)
- Zulfiqar B, Shelper TB, Avery VM. 2017. Leishmaniasis drug discovery: recent progress and challenges in assay development. *Drug Discov Today* 22:1516–1531. <https://doi.org/10.1016/j.drudis.2017.06.004>
- van der Ende J, Schallig H. 2023. *Leishmania* animal models used in drug discovery: a systematic review. *Animals (Basel)* 13:1650. <https://doi.org/10.3390/ani13101650>
- Mears ER, Modabber F, Don R, Johnson GE. 2015. A review: the current in vivo models for the discovery and utility of new anti-leishmanial drugs targeting cutaneous leishmaniasis. *PLoS Negl Trop Dis* 9:e0003889. <https://doi.org/10.1371/journal.pntd.0003889>
- Gopu B, Kour P, Pandian R, Singh K. 2023. Insights into the drug screening approaches in leishmaniasis. *Int Immunopharmacol* 114:109591. <https://doi.org/10.1016/j.intimp.2022.109591>
- Oliás-Molero AI, de la Fuente C, Cuquerella M, Torrado JJ, Alunda JM. 2021. Antileishmanial drug discovery and development: time to reset the model? *Microorganisms* 9:12. <https://doi.org/10.3390/microorganisms9122500>
- Neal RA, Croft SL. 1984. An *in-vitro* system for determining the activity of compounds against the intracellular amastigote form of *Leishmania donovani*. *J Antimicrob Chemother* 14:463–475. <https://doi.org/10.1093/jac/14.5.463>

12. Siqueira-Neto JL, Moon S, Jang J, Yang G, Lee C, Moon HK, Chatelain E, Genovesio A, Cechetto J, Freitas-Junior LH. 2012. An image-based high-content screening assay for compounds targeting intracellular *Leishmania donovani* amastigotes in human macrophages. *PLoS Negl Trop Dis* 6:e1671. <https://doi.org/10.1371/journal.pntd.0001671>
13. Okuno T, Goto Y, Matsumoto Y, Otsuka H, Matsumoto Y. 2003. Applications of recombinant *Leishmania amazonensis* expressing eGFP or the beta-galactosidase gene for drug screening and histopathological analysis. *Exp Anim* 52:109–118. <https://doi.org/10.1538/expanim.52.109>
14. Zhu X, Pandharkar T, Werbovets K. 2012. Identification of new antileishmanial leads from hits obtained by high-throughput screening. *Antimicrob Agents Chemother* 56:1182–1189. <https://doi.org/10.1128/AAC.05412-11>
15. Gupta S, Sundar S, Goyal N. 2005. Use of *Leishmania donovani* field isolates expressing the luciferase reporter gene in *in vitro* drug screening. *Antimicrob Agents Chemother* 49:3776–3783. <https://doi.org/10.1128/AAC.49.9.3776-3783.2005>
16. Singh N, Gupta R, Jaiswal AK, Sundar S, Dube A. 2009. Transgenic *Leishmania donovani* clinical isolates expressing green fluorescent protein constitutively for rapid and reliable *ex vivo* drug screening. *J Antimicrob Chemother* 64:370–374. <https://doi.org/10.1093/jac/dkp206>
17. Romanha AJ, Castro S de, Soeiro M de N, Lannes-Vieira J, Ribeiro I, Talvani A, Bourdin B, Blum B, Olivieri B, et al. 2010. *In vitro* and *in vivo* experimental models for drug screening and development for chagas disease. *Mem Inst Oswaldo Cruz* 105:233–238. <https://doi.org/10.1590/s0074-02762010000200022>
18. Gopu B, Kour P, Pandian R, Singh K. 2023. Insights into the drug screening approaches in leishmaniasis. *Int Immunopharmacol* 114:109591. <https://doi.org/10.1016/j.intimp.2022.109591>
19. Naylor LH. 1999. Reporter gene technology: the future looks bright. *Biochem Pharmacol* 58:749–757. [https://doi.org/10.1016/s0006-2952\(99\)00096-9](https://doi.org/10.1016/s0006-2952(99)00096-9)
20. Bastos MSE, Souza L de, Onofre TS, Silva A, Almeida M de, Bressan GC, Fietto JLR. 2017. Achievement of constitutive fluorescent pLEXSY-eGFP *Leishmania braziliensis* and its application as an alternative method for drug screening *in vitro*. *Mem Inst Oswaldo Cruz* 112:155–159. <https://doi.org/10.1590/0074-02760160237>
21. Bolhassani A, Taheri T, Taslimi Y, Zamanilui S, Zahedifard F, Seyed N, Torkashvand F, Vaziri B, Rafati S. 2011. Fluorescent leishmania species: development of stable GFP expression and its application for *in vitro* and *in vivo* studies. *Exp Parasitol* 127:637–645. <https://doi.org/10.1016/j.exppara.2010.12.006>
22. Dube A, Gupta R, Singh N. 2009. Reporter genes facilitating discovery of drugs targeting protozoan parasites. *Trends Parasitol* 25:432–439. <https://doi.org/10.1016/j.pt.2009.06.006>
23. Gupta S, Nishi. 2011. Visceral leishmaniasis: experimental models for drug discovery. *Indian J Med Res* 133:27–39. https://journals.lww.com/ijmr/Fulltext/2011/33010/Visceral_leishmaniasis__Experimental_models_for.6.aspx
24. Li F, Yang M, Wang L, Williamson I, Tian F, Qin M, Shah PK, Sharifi BG. 2012. Autofluorescence contributes to false-positive intracellular Foxp3 staining in macrophages: a lesson learned from flow cytometry. *J Immunol Methods* 386:101–107. <https://doi.org/10.1016/j.jim.2012.08.014>
25. Shaner NC, Steinbach PA, Tsien RY. 2005. A guide to choosing fluorescent proteins. *Nat Methods* 2:905–909. <https://doi.org/10.1038/nmeth819>
26. Canavaci AMC, Bustamante JM, Padilla AM, Perez Brandan CM, Simpson LJ, Xu D, Boehlke CL, Tarleton RL. 2010. *In vitro* and *in vivo* high-throughput assays for the testing of anti-*Trypanosoma cruzi* compounds. *PLoS Negl Trop Dis* 4:e740. <https://doi.org/10.1371/journal.pntd.0000740>
27. Winnard PT, Kluth JB, Raman V. 2006. Noninvasive optical tracking of red fluorescent protein-expressing cancer cells in a model of metastatic breast cancer. *Neoplasia* 8:796–806. <https://doi.org/10.1593/neo.06304>
28. Kumari S, Kumar V, Tiwari RK, Ravidas V, Pandey K, Kumar A. 2022. Amphotericin B: a drug of choice for visceral Leishmaniasis. *Acta Trop* 235:106661. <https://doi.org/10.1016/j.actatropica.2022.106661>
29. Balasegaram M, Ritmeijer K, Lima MA, Burza S, Ortiz Genovese G, Milani B, Gaspani S, Potet J, Chappuis F. 2012. Liposomal amphotericin B as a treatment for human leishmaniasis. *Expert Opin Emerg Drugs* 17:493–510. <https://doi.org/10.1517/14728214.2012.748036>
30. Machado PR, Ampuero J, Guimarães LH, Villasboas L, Rocha AT, Schriefer A, Sousa RS, Talhari A, Penna G, Carvalho EM, Buffet P. 2010. Miltefosine in the treatment of cutaneous leishmaniasis caused by *Leishmania braziliensis* in Brazil: a randomized and controlled trial. *PLoS Negl Trop Dis* 4:e912. <https://doi.org/10.1371/journal.pntd.0000912>
31. Unger C, Damenz W, Fleer EA, Kim DJ, Breiser A, Hilgard P, Engel J, Nagel G, Eibl H. 1989. Hexadecylphosphocholine, a new ether lipid analogue. studies on the antineoplastic activity *in vitro* and *in vivo*. *Acta Oncol* 28:213–217. <https://doi.org/10.3109/02841868909111249>
32. Martinez S, Gonzalez M, Vernaza ME. 1997. Treatment of cutaneous leishmaniasis with allopurinol and stibogluconate. *Clin Infect Dis* 24:165–169. <https://doi.org/10.1093/clinids/24.2.165>
33. Evans AT, Croft SL, Peters W. 1988. Failure of chlorpromazine or amitriptyline ointments to influence the course of experimental cutaneous leishmaniasis. *Trans R Soc Trop Med Hyg* 82:226. [https://doi.org/10.1016/0035-9203\(88\)90420-8](https://doi.org/10.1016/0035-9203(88)90420-8)
34. Cunha-Júnior EF, Andrade-Neto VV, Lima ML, da Costa-Silva TA, Galisteo Junior AJ, Abengózar MA, Barbas C, Rivas L, Almeida-Amaral EE, Tempone AG, Torres-Santos EC, Pollastri MP. 2017. Cyclobenzaprime raises ROS levels in *Leishmania infantum* and reduces parasite burden in infected mice. *PLoS Negl Trop Dis* 11:e0005281. <https://doi.org/10.1371/journal.pntd.0005281>
35. Zilberstein D, Liveanu V, Gepstein A. 1990. Tricyclic drugs reduce proton motive force in *Leishmania donovani* promastigotes. *Biochem Pharmacol* 39:935–940. [https://doi.org/10.1016/0006-2952\(90\)90210-c](https://doi.org/10.1016/0006-2952(90)90210-c)
36. Moreira D de S, Xavier MV, Murta SMF. 2018. Ascorbate peroxidase overexpression protects *Leishmania braziliensis* against trivalent antimony effects. *Mem Inst Oswaldo Cruz* 113:e180377. <https://doi.org/10.1590/0074-02760180377>
37. Moreira DS, Murta SMF. 2016. Involvement of nucleoside diphosphate kinase B and elongation factor 2 in *Leishmania braziliensis* antimony resistance phenotype. *Parasit Vectors* 9:641. <https://doi.org/10.1186/s13071-016-1930-6>
38. Abok K, Cadenas E, Brunk U. 1988. An experimental model system for leishmaniasis. effects of porphyrin-compounds and menadione on *Leishmania* parasites engulfed by cultured macrophages. *APMIS* 96:543–551. <https://doi.org/10.1111/j.1699-0463.1988.tb05342.x>
39. Ribeiro JM, Rodrigues-Alves ML, Oliveira E, Guimarães PPG, Maria Murta Santi A, Teixeira-Carvalho A, Murta SMF, Peruhype-Magalhães V, Souza-Fagundes EM. 2022. Pamidronate, a promising repositioning drug to treat leishmaniasis, displays antileishmanial and immunomodulatory potential. *Int Immunopharmacol* 110:108952. <https://doi.org/10.1016/j.intimp.2022.108952>
40. Piccica M, Lagi F, Bartoloni A, Zammarchi L. 2021. Efficacy and safety of pentamidine isethionate for tegumentary and visceral human leishmaniasis: a systematic review. *J Travel Med* 28:taab065. <https://doi.org/10.1093/jtm/taab065>
41. Nguewa PA, Fuertes MA, Cepeda V, Iborra S, Carrión J, Valladares B, Alonso C, Pérez JM. 2005. Pentamidine is an antiparasitic and apoptotic drug that selectively modifies ubiquitin. *Chem Biodivers* 2:1387–1400. <https://doi.org/10.1002/cbdv.200590111>
42. Miguel DC, Yokoyama-Yasunaka JKU, Uliana SRB. 2008. Tamoxifen is effective in the treatment of *Leishmania amazonensis* infections in mice. *PLoS Negl Trop Dis* 2:e249. <https://doi.org/10.1371/journal.pntd.0000249>
43. Miguel DC, Zauli-Nascimento RC, Yokoyama-Yasunaka JKU, Katz S, Barbiéri CL, Uliana SRB. 2009. Tamoxifen as a potential antileishmanial agent: efficacy in the treatment of *Leishmania braziliensis* and *Leishmania chagasi* infections. *J Antimicrob Chemother* 63:365–368. <https://doi.org/10.1093/jac/dkn509>
44. Barreto IM, Moreira POL, de Macedo GEL, Maia DNB, de Almeida Alves TM, de Oliveira DM, Cota BB. 2021. β -carboline glucoalkaloids from *Psychotria cupularis* and evaluation of their antileishmanial activity. *Rev Bras Farmacogn* 31:709–714. <https://doi.org/10.1007/s43450-021-00197-8>
45. Cota BB, Tunes LG, Maia DNB, Ramos JP, Oliveira D de, Kohlhoff M, Alves T de A, Souza-Fagundes EM, Campos FF, Zani CL. 2018. Leishmanicidal compounds of *Nectria pseudotrichia*, an endophytic fungus isolated from

- the plant *Caesalpinia echinata* (Brazilwood). Mem Inst Oswaldo Cruz 113:102–110. <https://doi.org/10.1590/0074-02760170217>
46. Siqueira EP, Oliveira DM, Johann S, Cisalpino PS, Cota BB, Rabello A, Alves TMA, Zani CL. 2011. Bioactivity of the compounds isolated from *Blepharocalyx salicifolius*. Rev bras farmacogn 21:645–651. <https://doi.org/10.1590/S0102-695X2011005000111>
47. Leverrier A, Bero J, Frédéric M, Quetin-Leclercq J, Palermo J. 2013. Antiparasitic hybrids of *Cinchona alkaloids* and bile acids. Eur J Med Chem 66:355–363. <https://doi.org/10.1016/j.ejmech.2013.06.004>
48. Marinho AMR, Marinho PSB, Santos LS, Filho ER, Ferreira ICP. 2011. Polyketides isolated from *Penicillium herquei*. Eclat Quím 36:38–45. <https://doi.org/10.1590/S0100-46702011000100003>
49. Fonseca-Silva F, Inacio JDF, Canto-Cavalheiro MM, Almeida-Amaral EE. 2011. Reactive oxygen species production and mitochondrial dysfunction contribute to quercetin induced death in *Leishmania amazonensis*. PLoS One 6:e14666. <https://doi.org/10.1371/journal.pone.0014666>
50. Cataneo AHD, Tomiotto-Pellissier F, Miranda-Sapla MM, Assolini JP, Panis C, Kian D, Yamauchi LM, Colado Simão AN, Casagrande R, Pinge-Filho P, Costa IN, Verri WA, Conchon-Costa I, Pavanelli WR. 2019. Quercetin promotes antipromastigote effect by increasing the ROS production and anti-amastigote by upregulating Nrf2/HO-1 expression, affecting iron availability. Biomed Pharmacother 113:108745. <https://doi.org/10.1016/j.biopha.2019.108745>
51. Lang T, Goyard S, Lebastard M, Milon G. 2005. Bioluminescent *Leishmania* expressing luciferase for rapid and high throughput screening of drugs acting on amastigote-harboring macrophages and for quantitative real-time monitoring of parasitism features in living mice. Cell Microbiol 7:383–392. <https://doi.org/10.1111/j.1462-5822.2004.00468.x>
52. Calvo-Alvarez E, Cren-Travaillé C, Crouzols A, Rotureau B. 2018. A new chimeric triple reporter fusion protein as a tool for *in vitro* and *in vivo* multimodal imaging to monitor the development of African trypanosomes and *Leishmania* parasites. Infect Genet Evol 63:391–403. <https://doi.org/10.1016/j.meegid.2018.01.011>
53. Chan M-Y, Bulinski JC, Chang K-P, Fong D. 2003. A microplate assay for *Leishmania amazonensis* promastigotes expressing multimeric green fluorescent protein. Parasitol Res 89:266–271. <https://doi.org/10.1007/s00436-002-0706-4>
54. Ambient A, Woods KL, Cull B, Coombs GH, Mottram JC. 2011. Morphological events during the cell cycle of *Leishmania major*. Eukaryot Cell 10:1429–1438. <https://doi.org/10.1128/EC.05118-11>
55. Clos J, Grünebast J, Holm M. 2022. Promastigote-to-Amastigote conversion in *Leishmania* spp. a molecular view. Pathogens 11:1052. <https://doi.org/10.3390/pathogens11091052>
56. Njoroge JM, Mitchell LB, Centola M, Kastner D, Raffeld M, Miller JL. 2001. Characterization of viable autofluorescent macrophages among cultured peripheral blood mononuclear cells. Cytometry 44:38–44. [https://doi.org/10.1002/1097-0320\(20010501\)44:1<38::aid-cyto1080>3.0.co;2-t](https://doi.org/10.1002/1097-0320(20010501)44:1<38::aid-cyto1080>3.0.co;2-t)
57. Flynn M, Heale KA, Alisaraie L. 2017. Mechanism of off-target interactions and toxicity of tamoxifen and its metabolites. Chem Res Toxicol 30:1492–1507. <https://doi.org/10.1021/acs.chemrestox.7b00112>
58. Bazvand F, Mahdizad Z, Mohammadi N, Shahi F, Mirghorbani M, Riazi-Esfahani H, Modjtahedi BS. 2023. Tamoxifen retinopathy. Surv Ophthalmol 68:628–640. <https://doi.org/10.1016/j.survophthal.2023.02.003>
59. Wang Z-F, Sun Z-C, Xiao L, Zhou Y-M, Du F-Y. 2019. Herbicidal polyketides and diketopiperazine derivatives from *Penicillium viridicatum*. J Agric Food Chem 67:14102–14109. <https://doi.org/10.1021/acs.jafc.9b06116>
60. Patel MR, Chang Y-F, Chen IY, Bachmann MH, Yan X, Contag CH, Gambhir SS. 2010. Longitudinal, noninvasive imaging of T-cell effector function and proliferation in living subjects. Cancer Res 70:10141–10149. <https://doi.org/10.1158/0008-5472.CAN-10-1843>
61. Robinson KA, Beverley SM. 2003. Improvements in transfection efficiency and tests of RNA interference (RNAi) approaches in the protozoan parasite *Leishmania*. Mol Biochem Parasitol 128:217–228. [https://doi.org/10.1016/s0166-6851\(03\)00079-3](https://doi.org/10.1016/s0166-6851(03)00079-3)
62. Coelho GS, Andrade JS, Xavier VF, Sales Junior PA, Rodrigues de Araujo BC, Fonseca K da S, Caetano MS, Murta SMF, Vieira PM, Carneiro CM, Taylor JG. 2019. Design, synthesis, molecular Modelling, and *in vitro* evaluation of tricyclic coumarins against *Trypanosoma cruzi*. Chem Biol Drug Des 93:337–350. <https://doi.org/10.1111/cbdd.13420>